Development of a Cell-Based, High-Throughput Screening Assay for Cholesterol Efflux Using a Fluorescent Mimic of Cholesterol

Jun Zhang,[1,2] Sutang Cai,[3] Blake R. Peterson,[3] Penny M. Kris-Etherton,[1,2] and John P. Vanden Heuvel[1,2,4]

[1]Department of Nutritional Sciences and [2]Center of Excellence in Nutrigenomics, The Pennsylvania State University, University Park, Pennsylvania.
[3]Department of Medicinal Chemistry, The University of Kansas, Lawrence, Kansas.
[4]Department of Veterinary and Biomedical Sciences, The Pennsylvania State University, University Park, Pennsylvania.

ABSTRACT

Reverse cholesterol transport is the process by which extrahepatic cells, including macrophage-derived foam cells in arterial atherosclerotic plaque, transport excessive cholesterol back to the liver for bile acid synthesis and excretion, thus lowering the peripheral lipid burden. Cholesterol efflux from peripheral cells is the first step in this process, and finding drugs and interventions that promote this event is an important endeavor. Radioisotope-labeled cholesterol traditionally has been employed in measuring efflux efficiency, but this reagent has limitations for high-throughput screening. We developed an alternative method to measure cholesterol efflux in macrophage-derived foam cells using a novel fluorescent cholesterol mimic comprising the Pennsylvania Green fluorophore, attached by a linker containing a glutamic acid residue, to a derivative of N-alkyl-3β-cholesterylamine. Compared with the traditional radioisotope-based assay, this fluorescence-based assay gave similar results in the presence of known modulators of cholesterol efflux, such as cyclic AMP, and different cholesterol acceptors. When the fluorescent probe was employed in a high-throughput screening format, a variety of chemicals and bioactive compounds with known and unknown effects on cholesterol efflux could be tested simultaneously by plate-reader in a short period of time. Treatment of THP-1-derived macrophages with inhibitors of the membrane transporter ATP-binding cassette A1, such as glyburide or a specific antibody, significantly reduced the export of this fluorescent compound, indicating that ATP-binding cassette A1 represents the primary mediator of its cellular efflux. This fluorescent mimic of cholesterol provides a safe, sensitive, and reproducible alternative to radioactive assays in efflux experiments and has great potential as a valuable tool when incorporated into a drug discovery program.
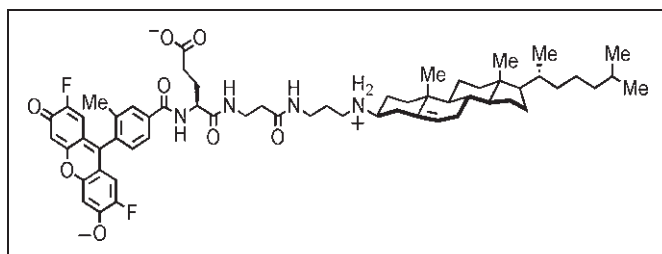
INTRODUCTION

Cardiovascular diseases (CVD) are one of the leading causes of morbidity and mortality worldwide. Numerous drug and dietary supplementation strategies have been developed to reduce the risk of CVD. A critically important intervention is to improve reverse cholesterol transport (RCT), a multi-step process in which excessive extrahepatic cholesterol is transported out of tissues and cells via the blood stream in the presence of lipid acceptors such as apolipoprotein A-I (apoA-I) or high-density lipoprotein (HDL).[1] The ultimate outcome of RCT is to bring peripheral cholesterol to the liver for excretion as bile acids, thus lowering the peripheral lipid burden and contributing to atherosclerosis regression.

Cholesterol efflux from peripheral tissues and cells such as macrophage-derived foam cells (MDFC) in atherosclerotic plaque is an initial and critical step in RCT. Enhancing cholesterol efflux is a leading mechanistic approach for drug therapies aimed at treating or preventing atherosclerosis and CVD. There are multiple interventions to increase cholesterol efflux within the foam cells, including, but not limited to, activating nuclear receptors (NRs) such as peroxisome proliferator-activated receptors (PPARs) and liver-X-receptors (LXRs).[2] These drug therapies increase expression of membrane transporters, such as ATP binding cassette (ABC) transporters, facilitating the transport of cholesterol across the plasma membrane.[3]

Although high-throughput screening (HTS) assays for these receptors and transporters have been developed, and can be used to identify anti-atherosclerosis therapies, examining the desired penultimate response (i.e., increased cholesterol efflux) is advantageous. Traditional methods to measure the effects of pharmaceutical agents on cholesterol efflux in in vitro models involve loading of MDFCs with radioisotope-labeled cholesterol. In the absence or presence of apoA-I or HDL, radioactivity in the medium relative to that in the cells is used to estimate the efficiency of cholesterol mobilization during the efflux

Fig. 1. Chemical structure of the fluorescent Pennsylvania Green/ *N*-alkyl-3β-cholesterylamine-derived molecular probe (F-Ch).

period. After treatment, the traditional efflux assay requires hours of incubation, scintillation counting, and cumbersome radioactivity disposal procedures, which limits its usefulness in many HTS applications.

In contrast, fluorescence-based assays are more amenable to screening programs. To explore this approach, we utilized a novel mimic of cholesterol comprising an *N*-alkyl-3β-cholesterylamine derivative linked to the fluorophore Pennsylvania Green via a linker containing a glutamic acid residue (*Fig. 1*; F-Ch). This compound is structurally similar to other previously reported cholesterylamine conjugates that are known to associate with cellular plasma membranes and selectively accumulate in early endosomes.[4] The Pennsylvania Green moiety is more hydrophobic, more photostable, and less pH sensitive than fluorescein, making it more useful for the construction of certain molecular probes of living cells. During a 24-h efflux period, pharmacologic agents modulated efflux of this fluorescent cholesterol mimic similarly compared to tritium-labeled cholesterol (^{3}H-Ch). After treatment with various RCT inducers, changes in efflux can be detected within an hour in a cell-based high-throughput format, indicating that F-Ch is a useful alternative probe for measurement of cholesterol efflux. In addition, by avoiding the need for detection and disposal of radioactivity, F-Ch is more easily incorporated into high- and medium-throughput screening drug discovery programs.

MATERIALS AND METHODS
Chemicals

The fluorescent Pennsylvania Green/*N*-alkyl-3β-cholesterylamine-derived probe (F-Ch) was synthesized by methods analogous to those reported previously.[4] Human low-density lipoprotein (LDL), ergosta-5,7,9(11),22-tetraen-3β-ol (dehydroergosterol; DHE), 8-Br cyclic AMP, palmitic acid, stearic acid, oleic acid, linoleic acid, α-linolenic acid (ALA), eicosapentaenoic acid, docosahexaenoic acid, sodium pyruvate, RPMI1640, phosphate-buffered saline (PBS), HEPES, 2-mecaptoethanol (2-ME), phorbol 12-myristate 13-acetate (PMA), ciprofibrate, TO901317, and GW4064 were purchased from Sigma-Aldrich (St. Louis, MO). Arachidonic acid, rosiglitazone, and 3-dodecanoyl-nitrobenzoxadiazole cholesterol (C12-NBD) were purchased from Cayman Chemical (Ann Arbor, MI). GW501516 and 9-cis retinoic acid was purchased from Enzo Life Sciences Inc. (Farmingdale, NY). 22-[*N*-(7-nitrobenz-2-oxa-1,3-diazol-4-yl)amino]-23,24-bisnor-5-cholen-3β-ol (22-NBD cholesterol) was purchased from Invitrogen (Carlsbad, CA). Lipid extracts of tree nuts were provided by the Food Analysis Laboratory Control Center, Virginia Polytechnic Institute and State University.[5]

Nut extracts were supplied in dimethyl sulfoxide (DMSO) as a stock concentration of 100 mg/mL. Fetal bovine serum (FBS) was purchased from Hyclone (Logan, UT). Rabbit polyclonal anti-ABCA1 antibody was purchased from Novus Biologicals Inc. (Littleton, CO). Rabbit polyclonal anti-ACTIN antibody was purchased from Santa Cruz Biotechnology Inc. (Santa Cruz, CA). Mouse monoclonal anti-glyceraldehyde 3-phosphate dehydrogenase antibody was purchased from Fitzgerald Industries International Inc. (Acton, MA). HDL and apoA-I were purchased from Calbiochem Biochemicals (La Jolla, CA). [1α,2α (n)-^{3}H] cholesterol was purchased from GE Healthcare Bio-Sciences Corp. (Piscataway, NJ).

Cell Culture

THP-1 (Homo sapiens monocyte) cell lines were obtained from the American Type Culture Collection (Rockville, MD). THP-1 monocytes were cultured in RPMI1640 with 10% heat-inactivated FBS, 50 μM 2-ME, 1 mM sodium pyruvate, and antibiotics. To differentiate THP-1 monocytes to macrophages, cells were incubated in the growth medium with addition of 100 nM PMA for 48 h lacking 2-ME.

Preparation of Oxidized LDL

LDL (200 μg protein/mL) was oxidized with 10 μM CuSO₄ at 37°C for 24 h. Oxidized LDL (oxLDL) was concentrated using Amicon Ultra centrifugal filter units (Millipore Corp., Billerica, MA). Excessive copper was removed by dialysis against 0.9% NaCl 3 times for 24 h at 4°C (Slide-A-Lyzer Mini Dialysis Units; Pierce, Rockford, IL) and was subsequently sealed under argon, stored at 4°C, and used within a month. Oxidation of fatty acids and protein components of LDL was determined by analyzing thiobarbituric acid reactive substances and agarose gel electrophoresis. Protein concentration of oxLDL was determined using the Bio-Rad DC protein assay (Bio-Rad Laboratories, Hercules, CA).

Cholesterol Efflux Assays

THP-1-derived macrophages were seeded in 24-well plates at a density of 3×10^5/well. To induce foam cell formation and label the intracellular cholesterol pool, cells were loaded with 50 μg/mL oxLDL and ^{3}H-Ch (1 μCi/mL) or F-Ch (10 μM) (from a 10 mM DMSO stock solution) in normal the growth medium. After 24 h, cells were washed twice with RPMI1640 and incubated in 1% FBS medium for another 10 to 12 h. This allowed the labeled cholesterol to be distributed to various intracellular compartments. The medium was subsequently discarded and cells were treated overnight with test compounds (16 to 18 h). Cells were then washed twice, and efflux was induced by addition of apoA-I or HDL at the indicated concentrations and times as shown in the figure legends. For the ^{3}H-Ch efflux experiment, the medium was collected at the designated times and centrifuged at 13,200 *g* for 10 min to remove cell debris. Cells were harvested by addition of lysis buffer (5 mM Tris HCl + 0.1% sodium dodecyl sulfate) and the medium, and intracellular tritium (cpm) was measured by liquid scintillation counting. The efflux ratio was calculated as: $100 \times \text{cpm}_{\text{Media}}/(\text{cpm}_{\text{Cell}} + \text{cpm}_{\text{Media}})$ %. For time-dependent efflux assays of F-Ch, the medium was collected at the indicated times and centrifuged at 13,200 *g* for 10 min to remove cell debris. Cells

were treated with lysis buffer, and the F-Ch in the medium was extracted with an equal volume of chloroform:methanol (3:1) to eliminate contributions from intrinsic medium fluorescence. Solvent was evaporated by centrifugation under vacuum and residual F-Ch was resuspended in ethanol. The F-Ch in the ethanol and cell lysates was quantified relative to individual standard curves using excitation and emission wavelengths of 485 and 535 nm, respectively. All assays of F-Ch were performed under conditions that minimize photobleaching.

HTS of Cholesterol Efflux

THP-1 monocytes in 96-well plates at a density of 1×10^5 cells/well were differentiated to macrophages by addition of 100 nM PMA for 48 h. After differentiation, cells were washed twice with PBS and cultured in the growth medium overnight. Foam cell induction and addition of the F-Ch probe were performed as described under Cholesterol Efflux Assays. After overnight treatment (16 to 18 h), cells were washed twice with PBS and incubated with 40 μg/mL apoA-I or 100 μg/mL HDL in PBS containing 0.2% bovine serum albumin (BSA) (a total volume of 120 μL/well) to induce efflux. After 1 h, 100 μL of the medium in each well was collected and transferred to a new 96-well plate by multi-channel pipette. Residual liquid in each well was removed by tapping. Cells were treated with 100 μL lysis buffer and homogenized on an orbital shaker for 10 min. Fluorescence from the PBS fraction and the cell lysate fraction were measured at excitation and emission wavelengths of 485 and 535 nm, repectively, relative to the values of standard curves. An HTS efflux assay protocol is provided in *Table 1*. The Z' Factor was calculated as $Z' = 1 - [(3SD of sample + 3SD of control)/(|mean of sample - mean of control|)]$ as described elsewhere.[6]

Table 1. High–Throughput Screening Efflux Assay Protocol in a 96–Well Plate Format			
Step	**Parameter**	**Value (μL)**	**Description**
Days 1–2	Plate and differentiate cells to macrophages	100	100,000/well with 100 nM PMA for 48 h
Day 3	Stop differentiation	100	Wash twice with RPMI 1640 and recover overnight in the growth medium
Day 4	Cholesterol load and label	100	50 μg/mL oxLDL and 10 μM F-Ch for 24 h
Day 5	Equilibrium	100	Discard the medium and incubate in 1% FBS for 10 to 12 h
	Treatment	100	After equilibrium, treat cells in 1% FBS for 16 to 18 h
Day 6	I. Stop treatment	I. 100	Wash twice with PBS
	II. Cholesterol efflux	II. 120	40 μg/mL apoA-I, 100 μg/mL HDL, 0.2% BSA in PBS for 1 h
	III. Measurement	III. 100	Ex/Em 485/535 nm
Step	**Notes**		
Days 1–2	Leave the 1st row empty and save for standard later.		
Day 3	Be gentle during wash, and tap clean the plate.		
Day 4	Avoid direct light exposure and cover the plate with foil (the same for days 5–6).		
Day 5	Discard the medium after equilibrium, tap clean the plate, and treat cells in 1% FBS.		
Day 6	I. Be gentle during wash and tap clean the plate.		
	II. Prepare stock solution of PBS and aliquot to each well with multi-channel pipette.		
	III. (1) Transfer 100 μL solution to a new plate with multi-channel pipette (leave the 1st row of the new plate empty for standard), aspirate the remaining PBS; add 100 μL lysis buffer to each well of cell plate. (2) Standard of PBS plate: start with 1 μM and series dilution 1:3. (3) Standard of cell plate: start with 40 μM and series dilution 1:2.		

For other macrophage cell lines not requiring differentiation, the assay can start from day 4 after seeding the cells in a 96-well plate.
apoA-I, apolipoprotein A-I; BSA, bovine serum albumin; FBS, fetal bovine serum; HDL, high-density lipoprotein; oxLDL, oxidized low-density lipoprotein; PBS, phosphate-buffered saline; PMA, phorbol 12-myristate 13-acetate.

Fig. 2. Comparison of time-dependent efflux of ^{3}H-Ch and F-Ch. **(A)** Efflux of ^{3}H-Ch during a 24-h period. **(B)** Efflux of F-Ch during a 24-h period. Efflux shown in **(A)** and **(B)** was induced by addition of 10 µg/mL apoA-I and samples were collected at the indicated times. **(C)** Efflux of ^{3}H-Ch during a 24-h period. **(D)** Efflux of F-Ch during a 24-h period. Efflux shown in **(C)** and **(D)** was induced by addition of 50 µg/mL HDL protein. All data were plotted by a non-linear regression/curve fitting method. Asterisk (*) indicates a significant difference between BSA and cAMP treatment at the designated time. The data presented are mean ± SEM values of triplicate wells. The results are representative of 3 independent experiments. apoA-I, apolipoprotein A-I; BSA, bovine serum albumin; HDL, high-density lipoprotein; ^{3}H-Ch, tritium-labeled cholesterol; SEM, standard error of the mean.
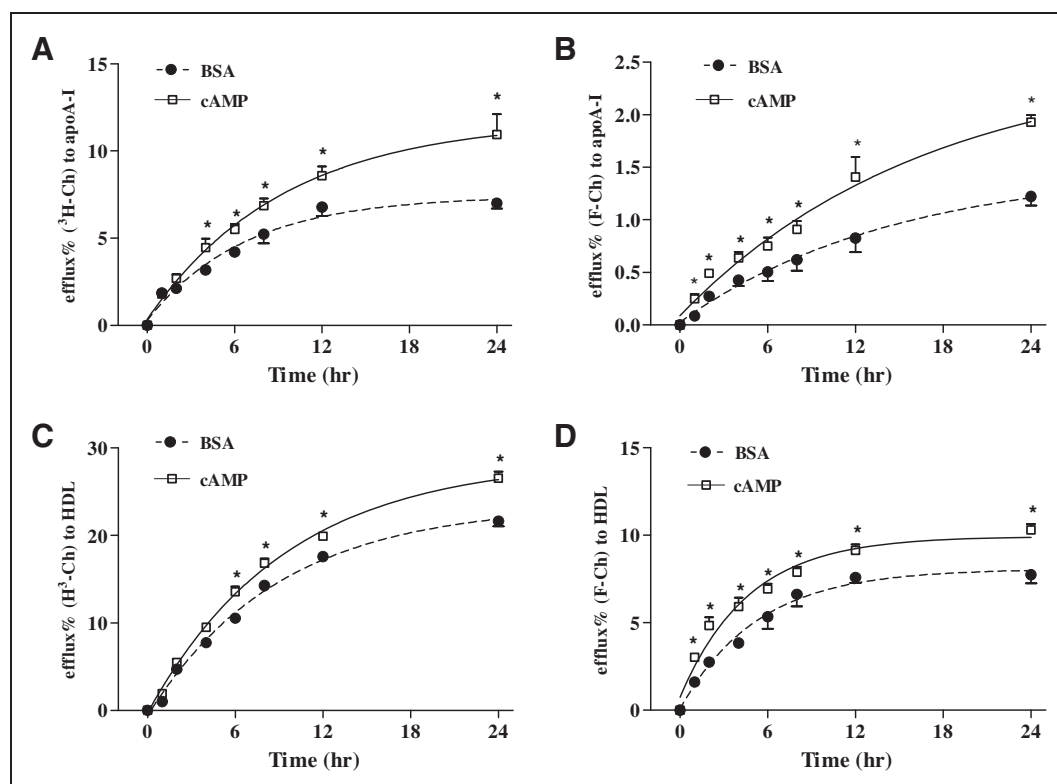
RNA Extraction, Reverse Transcription, and Real–Time Polymerase Chain Reaction

Cells were lysed and harvested using TriReagent according to the manufacturer's instructions (Sigma, St. Louis, MO). A high-capacity cDNA Archive kit (Applied Biosystems; Foster City, CA) was used for reverse transcription. About 20 ng/µL of cDNA was amplified by SYBR Green PCR Master Mix (Applied Biosystems) and detected by ABI 7300 Sequence Detection System (Applied Biosystems). Primer sequences are as follows—ABCA1: forward TGTGCAGATCATAGCCAAAAGC and reverse AGCCGCCATACCTAAACTCATT; ABCG1: forward CCCAGC AGATTTTGTCATGGA and reverse ACCAGCCGACTGTTCTGATCA; ABCA2: forward CCTGCCTCCCTTCCAGTGGGT and reverse TTCTG TCGCAGCCCCAGCAG; ABCA7: forward CTGGCCCAGGTCTCTGGCCT and reverse CCGTACTGGCCTGGGCACAC; ABCG4: forward GCGC GTCAAGGTCGGCG and reverse AGGTGCGTGGTCAGCACAGG.

Western Blot

THP-1 monocytes were seeded and differentiated to macrophages in 6-well plate at a density of 2×10^6/well. Macrophages were loaded with 50 µg/mL of oxLDL for 24 h, followed by treatment with cAMP overnight. Cells were collected in lysis buffer comprising 0.25 M sucrose, 10 mM Tris-acetate (pH 8.1), 1 mM EDTA, and 1 mM DTT. Cell lysates were sequentially centrifuged at 800 g and 13,200 g. Protein concentration was measured by Bio-Rad DC protein assay kit. Total soluble protein was separated on a 6% sodium dodecyl sulfate-polyacrylamide gel electrophoresis gel and transferred to a polyvinylidene fluoride membrane (Immobilon P; Millipore, Bedford, MA). Membranes were blotted in 5% nonfat milk in TBS+0.2% Tween 20 (TBS$^+$) at 4°C overnight and incubated with primary antibodies (anti-ABCA1 1:500) again at 4°C overnight. Membranes were washed 3 times with TBS$^+$ and incubated with horseradish peroxidase-linked secondary anti-rabbit antibody (1:10,000) for 1 h at room temperature. Blots were observed by ECL plus western blot detection kit (GE Healthcare Biosciences).

Statistical Analyses

Normality of the data was checked by Anderson–Darling test. General Linear Model analysis of variance, followed by Tukey *post-hoc* test, was used to test the difference between treatments ($P < 0.05$). The values were expressed as mean ± standard error of the mean. All data analyses were performed using Minitab Ver.15 (Minitab Inc., State College, PA) and data plotted by Prism 5.01 (GraphPad Software, Inc., San Diego, CA).

RESULTS
Efflux of F-Ch and ^{3}H-Ch Follows Similar Trends in MDFCs

To examine whether F-Ch could substitute for ^{3}H-Ch in quantitative cholesterol efflux assays, time-dependent fluorescent- and radioactive-based experiments were performed in THP-1 MDFC. Efflux of F-Ch and ^{3}H-Ch reached a peak at 24 h using either apoA-I or HDL as an inducer. When using ^{3}H-Ch as a tracer to measure apoA-I-induced cholesterol efflux, efflux was significantly increased between 4 h (1.7-fold) and 24 h (1.6-fold) after cAMP treatment, compared with a BSA control (*Fig. 2A*). In the fluorescence-based assay, cAMP also signif-

icantly increased apoA-I-induced efflux from MDFC (*Fig. 2B*). However, when using F-Ch as the tracer, the difference in efflux between treatment of BSA and cAMP was significant after 1 h (2.6-fold) through 24 h (1.6-fold), relative to a BSA control (*Fig. 2B*). Efflux of F-Ch and ^{3}H-Ch also was tested using HDL as a lipid acceptor in THP-1 MDFC. With ^{3}H-Ch, cAMP increased cholesterol efflux from 6 (1.3-fold) to 24 h (1.2-fold), compared to a BSA control (*Fig. 2C*). Efflux of F-Ch by cAMP was significantly increased at 1 h (1.9-fold), with continuously significant increases of efflux from 2 h (1.8-fold) to 24 h (1.3-fold), compared to a BSA control (*Fig. 2D*).

A Cell-Based Fluorescent Cholesterol Efflux Assay in a HTS Format

During a 24-h measurement interval, differences in the magnitude of efflux of F-Ch induced by apoA-I- and HDL were observed as early as 1 h postinduction. To avoid the solvent extraction and to utilize the fluorescence-based cholesterol efflux assay in a HTS format, different concentrations of apoA-I and HDL were applied to cAMP-treated cells in PBS for 1 h to test their efflux capability. ApoA-I (10 to 80 µg/mL) and HDL (50 to 200 µg/mL) increased cholesterol efflux in a dose-dependent manner in THP-1 MDFC (*Fig. 3A, B*). To evaluate the assay in a HTS format, cAMP was used as a positive control. Calculated Z'-factors were 0.54 and 0.57 for apoA-I- (40 µg/mL) and HDL- (100 µg/mL) induced efflux at 1 h, indicating that these are marginally robust assays (*Fig. 3C*). ApoA-I and HDL at lower concentrations did not appear to be suitable for high-throughput screens (data not shown). Intracellular F-Ch concentration was measured in this HTS format after nonacceptor- and acceptor-induced efflux. Cyclic AMP treatment significantly decreased intracellular F-Ch concentration in the absence of any acceptors (*Fig. 3D*). In the presence of apoA-I and HDL, the intracellular F-Ch concentration was further reduced after cAMP treatment, compared to respective controls (*Fig. 3D*). Thus, incorporation of this F-Ch in HTS program implies an easy and rapid alternative for measurement of cholesterol efflux.

The suitability and superiority of F-Ch to other fluorescent cholesterol derivatives (DHE, 22-NBD, and C12-NBD) in this assay was also tested in the same HTS format. In the absence of acceptors, efflux was significantly increased after cAMP treatment when cells were labeled with F-Ch, DHE, and C12-NBD cholesterol (*Fig. 3E*). In contrast, 22-NBD cholesterol did not show differences in efflux after treatment with the BSA control and cAMP. In the presence of apoA-I and HDL, a further increase of efflux after cAMP treatment was only observed in cells labeled with F-Ch (*Fig. 3F*). In our hands, at this early time-point, there was no difference in efflux between BSA and cAMP treatment when labeling cells with other fluorescent compounds (*Fig. 3F*). This indicates that the F-Ch tracer has superior attributes as a cholesterol mimic in this assay.

HTS to Identify Compounds That Affect Fluorescence-Based Cholesterol Efflux

NRs are intracellular proteins that interact with chemicals or dietary bioactives and regulate gene expression. Many drugs or dietary therapeutics affect cholesterol efflux through the action of NRs, by

which gene expression related to cholesterol storage and transport is changed. Multiple NR agonists with known and undefined effects on cholesterol efflux were examined. After treatment with the PPAR-γ agonist rosiglitazone (10, 3.3 µM), the LXR-α agonist T0901317 (5, 1.7 µM), the farnesoid-X-receptor (FXR)-α agonist GW4064 (10, 3.3 µM), or the pregnane-X-receptor (PXR) agonist rifampicin (50, 17 µM), F-Ch efflux was significantly increased (*Fig. 4A, C*). During the ^{3}H-Ch-based efflux measurement, these NR agonists induced similar increases in cholesterol efflux (*Fig. 4B, D*). Other tested NR agonists, ciprofibrate (the PPAR-α agonist), GW501506 (the PPAR-β agonist), and 9-cis retinoic acid (the RXR agonist), did not lead to a significant increase of cholesterol efflux (data not shown). Tree nut extracts and fatty acids, relatively mild effectors, also were applied to THP-1 MDFC to test their effect on efflux. Among the tree nut extracts, the walnuts extract showed significant effects on cholesterol efflux (14% to 22% increase) (*Fig. 4E*), whereas other nut extracts tested (Macadamia nut, Pine nut, Pecan, Pistachio, Cashew, and Hazelnut) did not significantly affect this process (data not shown). To identify lipid components that might contribute to the increased efflux, the effect of fatty acids on cholesterol efflux was tested. ALA, a predominant omega-3 polyunsaturated fatty acid in walnuts, significantly increased cholesterol efflux in the absence and presence of acceptors (*Fig. 4E*), whereas other unsaturated fatty acids (oleic acid, linoleic acid, and arachidonic acid) had no effect (data not shown). Walnuts extract and ALA treatment showed a similar percentage increase of cholesterol efflux when ^{3}H-Ch being as a probe (*Fig. 4F*). Collectively, these data showed that a variety of chemical compounds or complex mixtures can be analyzed simultaneously using this fluorescence-based assay incorporating F-Ch as a molecular probe.

The Membrane Transporter ABCA1 Facilitates the Efflux of the Fluorescent Cholesterol Mimic F-Ch

Members of the ABC family transporters facilitate the transport of a wide variety of molecules across the plasma membrane and are of critical importance in cholesterol efflux. ABCA1 is one of the mostly widely studied transporters, and its activity is dramatically increased by cAMP. After cAMP treatment, messenger RNAs of various ABC membrane transporters were measured. Among the tested transporters, ABCA1 had the highest expression level in THP-1 MDFCs, which was about 10-fold higher than ABCG1, and about 10,000-fold higher than ABCA2, ABCA7, and ABCG4 (data not shown). After cAMP treatment, ABCA1 mRNA and protein was elevated, whereas the change in ABCG1 was not significant (*Fig. 5A*). To investigate whether ABC transporters export F-Ch, the ABC transporter inhibitor glyburide (more specific to ABCA1) was applied. Without cAMP treatment, export of F-Ch only was significantly reduced at the highest glyburide concentration (500 µM) (*Fig. 5B, C*). After an overnight treatment with cAMP, cholesterol efflux was significantly increased by apoA-I and HDL in the absence of glyburide (2.9-fold and 2.1-fold increase, respectively) (*Fig. 5B, C*). Importantly, addition of glyburide (62.5 to 500 µM) significantly blunted apoA-I-induced efflux by 35% to 40% after cAMP treatment (*Fig. 5B*). HDL-induced cholesterol efflux was
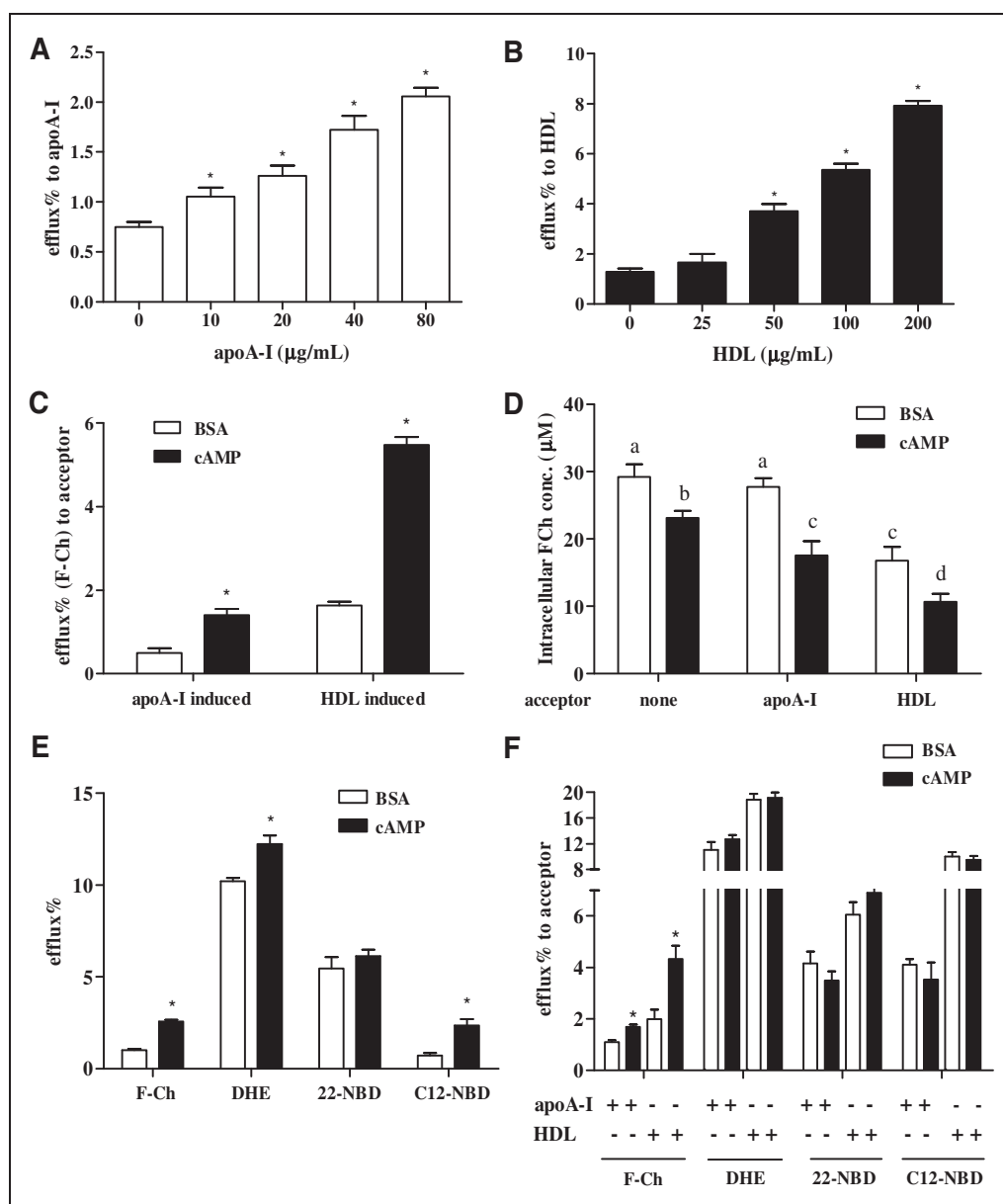
Fig. 3. Evaluation of F-Ch efflux in a high-throughput format. **(A)** Effect of various concentrations of apoA-I on cholesterol efflux after cAMP treatment. Asterisk (*) indicates a significant difference from the non-apoA-I group. **(B)** Effect of various concentrations of HDL on cholesterol efflux after cAMP treatment. Asterisk (*) indicates a significant difference from the non-HDL group. **(C)** Apo-AI-induced (40 μg/mL) and HDL-induced (100 μg/mL) efflux assay to examine utility in a high-throughput format. Asterisk (*) indicates a significant difference from the respective group. **(D)** Quantification of intracellular F-Ch after efflux under nonacceptor- and acceptor-induced (apoA-I 40 μg/mL and HDL 100 μg/mL) conditions. Bars not sharing common letters differ. **(E)** The difference in efflux between BSA control and cAMP in the absence of acceptor after cells were labeled with various fluorescent cholesterol derivatives (F-Ch 10 μg/mL; dehydroergosterol 10 μg/mL; 22-NBD 5 μg/mL; C12-NBD 2 μg/mL). Asterisk (*) indicates a significant difference from the respective group. **(F)** The difference in efflux between BSA control and cAMP in the presence of acceptor (apoA-I 40 μg/mL and HDL 100 μg/mL) after cells were labeled with various fluorescent cholesterol derivatives. Asterisk (*) indicates a significant difference from the respective group. The data presented are mean ± SEM values of triplicate wells. The results are representative of 2 independent experiments.
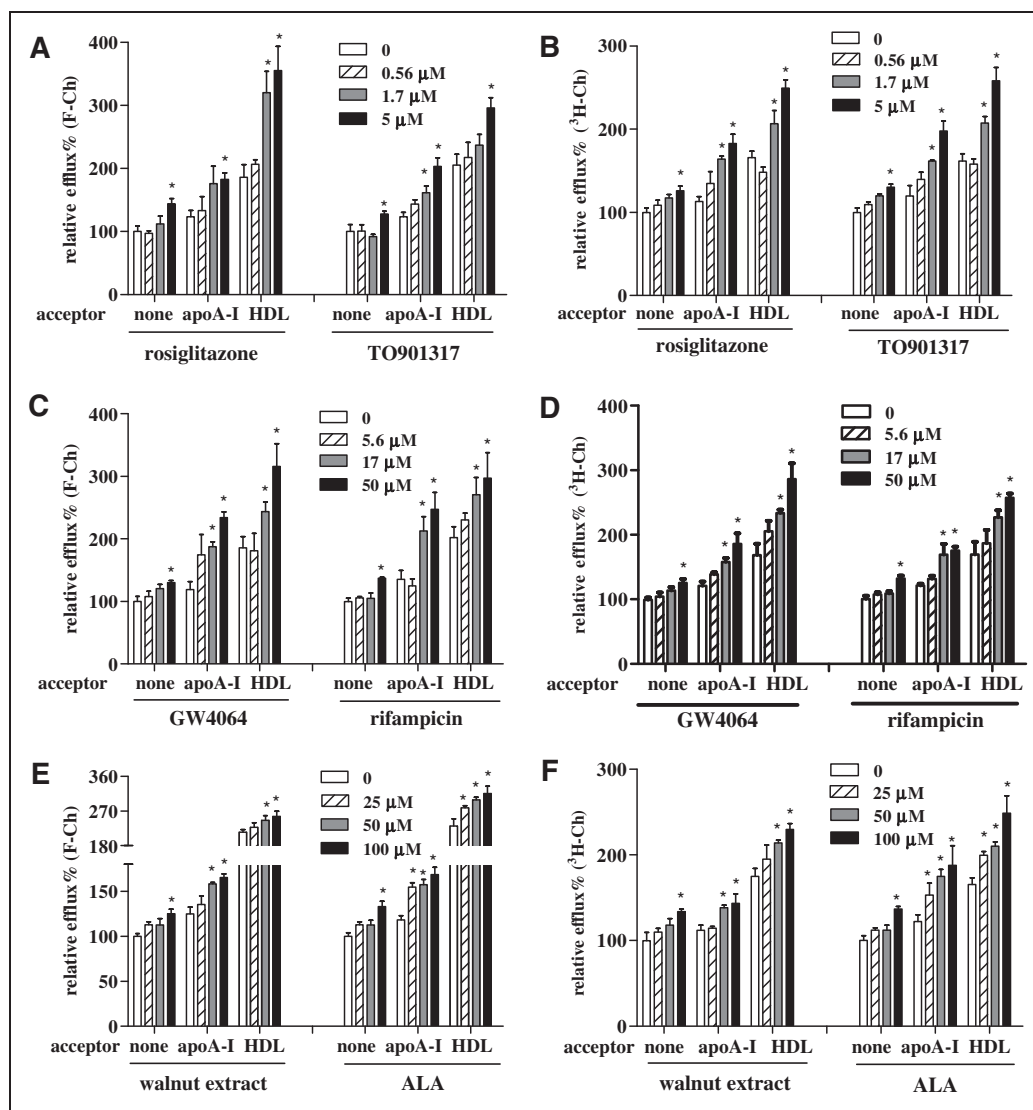
Fig. 4. Performance of F-Ch and ³H-Ch in a high-throughput cholesterol efflux assay. **(A)** Effects of NR agonists on nonacceptor and acceptor-induced cholesterol efflux. Cells were labeled with F-Ch and treated overnight with rosiglitazone (peroxisome proliferator-activated receptor-γ agonist) and TO901317 (liver-X-receptor agonist). **(B)** Effects of NR agonists on nonacceptor- and acceptor-induced cholesterol efflux. Cells were labeled with ³H-Ch and treated overnight with rosiglitazone and TO901317. **(C)** Effects of NR agonists on nonacceptor and acceptor-induced cholesterol efflux. Cells were labeled with F-Ch and treated overnight with GW4064 (farnesoid-X-receptor [FXR] agonist) and rifampicin (pregnane-X-receptor [PXR] agonist). **(D)** Effects of NR agonists on nonacceptor and acceptor-induced cholesterol efflux. Cells were labeled with ³H-Ch and treated overnight with GW4064 and rifampicin. **(E)** Effects of walnut lipid extract and its omega-3 polyunsaturated fatty acid ALA on nonacceptor and acceptor-induced cholesterol efflux. Cells were labeled with F-Ch and treated overnight with walnuts extract and ALA. NR agonists and tree nuts extracts were dissolved in DMSO. Fatty acid (ALA) was conjugated to BSA at a molar ratio of 4:1 based on the method described by Calder *et al.*[39] **(F)** Effects of walnut lipid extract and its omega-3 polyunsaturated fatty acid ALA on nonacceptor- and acceptor-induced cholesterol efflux. Cells were labeled with ³H-Ch and treated overnight with walnuts extract and ALA. The efflux values of nonacceptor controls were normalized to a value of 100%. All other efflux values are expressed relative to the value of nonacceptor control. Asterisk (*) indicates a significant difference between treatment and respective controls (nonacceptor, apoA-I, and HDL groups). The data presented are mean ± SEM values of triplicate wells. The results are representative of 2 independent experiments. NR, nuclear receptor.

reduced by 23% to 33% in the presence of glyburide (*Fig. 5C*). In the ³H-Ch-based efflux assay, only the highest concentration of glyburide inhibited the export of ³H-Ch in the absence of cAMP treatment, similar to the results with F-Ch (data not shown). ApoA-I- and HDL-induced ³H-Ch efflux was significantly decreased by

26% to 42% (*Fig. 5D*) and 22% to 27% (*Fig. 5E*), respectively, when cells were co-treated with glyburide. Although the glyburide experiments suggest that F-Ch is transported via ABCA1, a specific neutralizing antibody to this protein was also examined to further confirm the involvement of this transporter. Importantly, when the
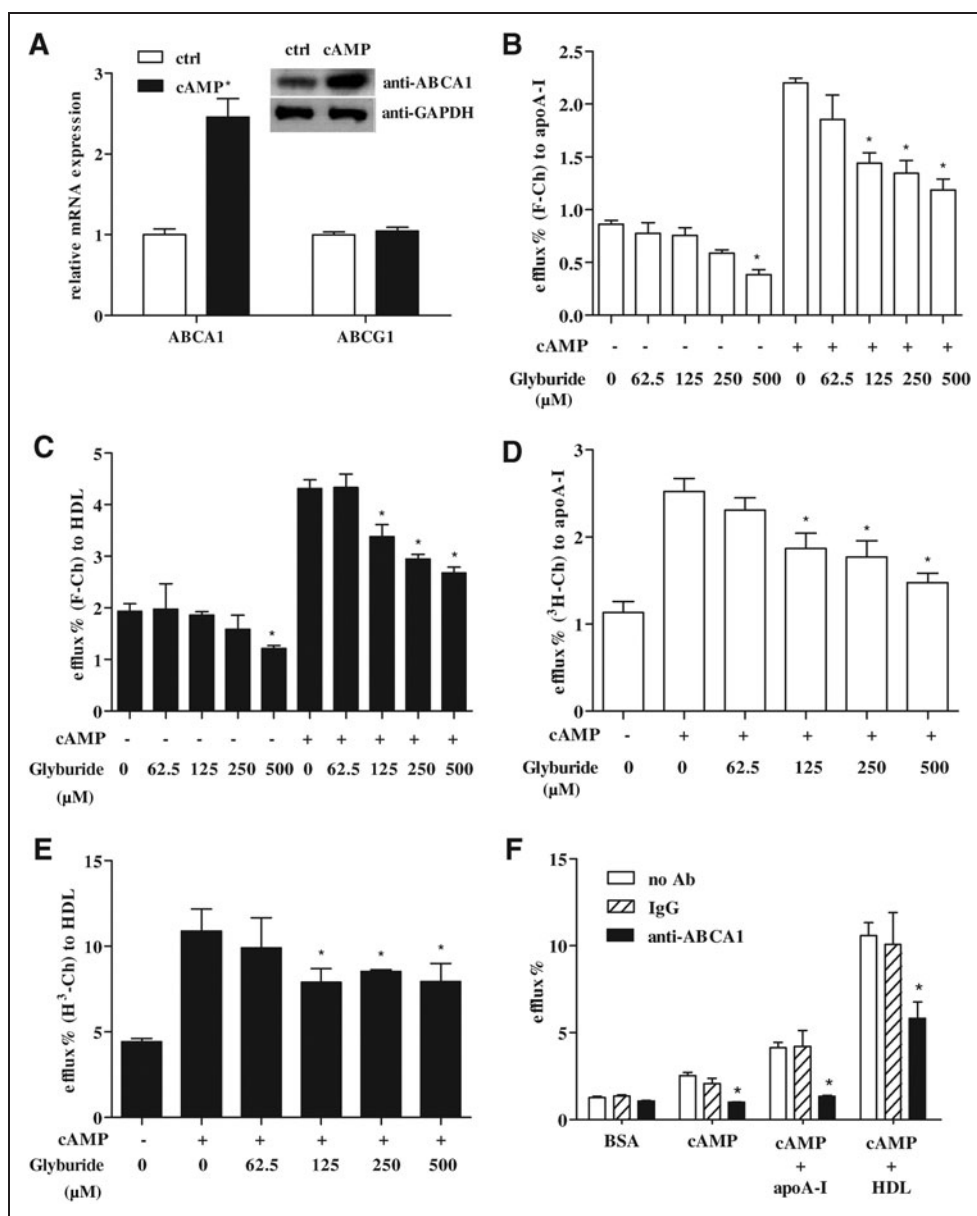
Fig. 5. F-Ch is exported across the plasma membrane by the ABCA1 transporter. **(A)** Messenger RNA of ABCA1, ABCG1, and ABCA1 protein in THP-1-derived foam cells after cAMP treatment ($300\,\mu M$). Asterisk (*) indicates a significant difference from BSA control. **(B)** Effect of glyburide on apoA-I-induced efflux of F-Ch. Asterisk (*) indicates a significant difference from the $0\,\mu M$ glyburide group. **(C)** Effect of glyburide on HDL-induced efflux of F-Ch. Asterisk (*) indicates a significant difference from the $0\,\mu M$ glyburide group. **(D)** Effect of glyburide on apoA-I-induced efflux of ^{3}H-Ch. Asterisk (*) indicates a significant difference from the $0\,\mu M$ glyburide group. **(E)** Effect of glyburide on HDL-induced efflux of ^{3}H-Ch. Asterisk (*) indicates a significant difference from the $0\,\mu M$ glyburide group. Efflux shown in **(B)** and **(D)** was induced by addition of $40\,\mu g/mL$ apoA-I for 1 h in phosphate-buffered saline. Efflux shown in **(C)** and **(E)** was induced by addition of $100\,\mu g/mL$ HDL for 1 h in phosphate-buffered saline. **(F)** Specific inhibition of ABCA1 decreases F-Ch efflux from THP-1-derived foam cells. Rabbit polyclonal anti-ACTIN antibody was used as a control. Rabbit polyclonal anti-ABCA1 antibody (1:200) was co-treated with cAMP overnight and was present during the efflux period. Asterisk (*) indicates a significant difference from controls. The data presented are mean ± SEM values of triplicate wells. The results are representative of 2 independent experiments. ABC, ATP binding cassette.

cells were incubated with anti-ABCA1 antibody, the cAMP-induced efflux of F-Ch was significantly decreased, both in the absence and presence of acceptors (*Fig. 5F*).

DISCUSSION

Peripheral cholesterol efflux, an initial step in RCT, is critically important for the prevention of atherosclerosis. Therapeutics that decreases the lipid-load of atherosclerotic plaque can prevent plaque rupture and reduce the incidence of heart attack and stroke. Identification of drugs and bioactive compounds that contribute to the regression of atherosclerosis is an important endeavor to enhance human health. However, traditional methods for measurement of cholesterol efflux using radioactive labeling have limited utility for HTS. We report herein that a new fluorescent mimic of cholesterol comprising Pennsylvania Green linked to an *N*-alkyl-3β-cholesterylamine via a linker containing glutamic acid can function similarly to traditional ^{3}H-Ch for measurement of cholesterol efflux. Although the mechanism of efflux between these 2 tracers appears to be similar, the extent of export quantified using F-Ch was somewhat smaller than that of ^{3}H-Ch, for several reasons. First, the molecular weight of fluorescent mimic is over twice that of cholesterol. The size and charged groups of F-Ch may lead to different transport dynamics across membranes from that of ^{3}H-Ch, which may explain the time-course differences in export observed. Second, F-Ch is not only actively associated with plasma membrane but also accumulates in early endosomes, and localization in these compartments may affect its rate of export. Third, there are alternative methods of probe measurement, each with different sensitivities and caveats that must be considered.

One such confounding issue that can affect fluorescent-based measurements is quenching of the signal by components in the medium; thus, a solvent extraction step for the time-dependent assay with F-Ch can be beneficial. However, this additional step can be overcome in HTS assays by utilizing an alternative medium that does not interfere with the fluorescent signal. Modification of this longer duration protocol by using a 1-h measurement in PBS can alternatively be used to omit the extra extraction step. Efflux measurements with F-Ch appeared to be more sensitive than the radioactive probe because significant differences in efflux could be observed after only a 1-h period. When applied as a tool for HTS, this assay can be used to simultaneously screen multiple chemicals for effects on cholesterol efflux, save labor-intensive sample preparation for scintillation counting, significantly shorten sample reading time, and avoid the need to dispose of radioactive waste.

Other fluorescent cholesterol derivatives have been utilized to examine intracellular sterol trafficking. DHE is a naturally occurring fluorescent cholesterol analog (in yeast) differing from cholesterol only in having 3 additional double bonds and an extra methyl group. DHE mimics the behavior of radiolabeled cholesterol in some studies,[7,8] and can serve as a replacement of up to 85% of the endogenous sterol of cultured fibroblasts. Despite characterization of DHE and its use in fluorescence spectroscopic studies, the difficulty in imaging DHE comes from the fact that it absorbs in the UV region of the spectrum and is highly susceptible to photobleaching. Alternatively, NBD fluorophores exhibit a high quantum yield and reasonably good photostability in hydrophobic environments. The 22- or 25-NBD sterols differ in the position of the fluorophore attached to the side chain of cholesterol. Some studies have shown that NBD-tagged sterols can be useful tools to investigate intracellular cholesterol trafficking and membrane function.[9-12] C12-NBD cholesterol has a hydrophilic NBD fluorophore attached to the hydrophilic end of cholesterol, separated by a 12-carbon spacer and has been used to measure cholesterol efflux.[13] However, in our HTS format, F-Ch is the only tested compound that demonstrated increased efflux in the absence and presence of lipid acceptors in this rapid (1 h) protocol. Obviously, due to the differences in structure of the cholesterol tracers, each has different orientations in the bilayer membrane, and interactions with other intracellular protein(s),[14] which can result in different membrane trafficking dynamics.

To screen chemicals against this novel fluorescence-based assay in a HTS format, bioactive compounds with both known and unknown effects on cholesterol efflux were examined at various concentrations. Cells were treated with NR agonists to probe potential mechanisms of action. The PPAR-γ agonist rosiglitazone and the LXR-α agonist TO901317 were found to significantly increase cholesterol efflux, consistent with previous reports (reviewed by Duffy and Rader[15]). Interestingly, GW4064, a synthetic FXR agonist, and rifampicin, a PXR agonist, also significantly increased cholesterol efflux. Although the anti-atherogenic effects of FXR and PXR agonists are not clear,[16-18] the underlying mechanisms of this activity may warrant further exploration.

Besides synthetic chemicals with potent effects on induction of efflux, mild compounds/complexes also were applied to this type of assay. Intake of tree nuts has hypocholesterolemic effects in different populations[19]; however, little is known about their anti-atherogenic properties. Among the tested tree nut extracts, only the walnut lipid extract significantly increased cholesterol efflux. Previous studies have shown that walnut intake can favorably affect lipid and lipoprotein profiles,[20] inhibit cytokine release,[21,22] and favorably affect atherosclerosis risk factors. Walnut is a tree nut unique in its fatty acid profile, and it is especially rich in plant-derived omega-3 polyunsaturated fatty acid, ALA.[19] To clarify the lipid components in the walnut extract that induce efflux, major saturated, omega-9, omega-6, and omega-3 unsaturated fatty acids[23] were tested. The results indicated that ALA significantly increase cholesterol efflux compared with the BSA control. The presence of ALA in walnut might explain the increased cholesterol efflux observed in the lipid extract. In addition, eicosapentaenoic acid and docosahexaenoic acid, the marine-derived omega-3 fatty acids, also significantly increased cholesterol efflux (data not shown). The results were consistent with the anti-atherogenic effect of fish oil in several studies.[24,25]

Cyclic AMP was applied in efflux experiments as a positive control since it induces expression of ABC transporters at the plasma membrane.[26-29] The 2 major membrane transporters, ABCA1 and ABCG1, of macrophages are known[30,31] to unidirectionally export intracellular

free cholesterol to extracellular acceptors, such as apoA-I or HDL. Glyburide blocks membrane ABC transporters, especially ABCA1, thus decreasing cholesterol efflux.[32,33] In the study presented herein, glyburide significantly reduced apoA-I-and HDL-induced cholesterol efflux, suggesting that the efflux of both F-Ch and ^{3}H-Ch is mediated by the same ABCA1 transporters. However, since other ABC family members, such as ABCA2, ABCA7, ABCG1, and ABCG4, also play roles in lipid trafficking[34–38] and glyburide's specificity is in doubt, a more specific method of inhibition, a neutralizing antibody to ABCA1, was also examined. These experiments clearly demonstrate that ABCA1 is the predominant transporter of F-Ch from MDFCs.

In conclusion, the novel fluorescence-based assay reported herein provides a simple and sensitive alternative to existing radioactive methods for measuring cholesterol efflux that mimics the transport of lipid from MDFCs.

ACKNOWLEDGMENTS

AUTHOR DISCLOSURE STATEMENT

J.Z., P.M.K.-E., and J.P.V.H. are employees of Pennsylvania State University. S.C. and B.R.P. are employees of the University of Kansas.

REFERENCES

1. Chapman MJ: Therapeutic elevation of HDL-cholesterol to prevent atherosclerosis and coronary heart disease. *Pharmacol Ther* 2006;111:893–908.

2. Rigamonti E, Chinetti-Gbaguidi G, Staels B: Regulation of macrophage functions by PPAR-alpha, PPAR-gamma, and LXRs in mice and men. *Arterioscler Thromb Vasc Biol* 2008;28:1050–1059.

3. Tall AR, Yvan-Charvet L, Terasaka N, Pagler T, Wang N: HDL, ABC transporters, and cholesterol efflux: implications for the treatment of atherosclerosis. *Cell Metab* 2008;7:365–375.

4. Mottram LF, Boonyarattanakalin S, Kovel RE, Peterson BR: The Pennsylvania Green Fluorophore: a hybrid of Oregon Green and Tokyo Green for the construction of hydrophobic and pH-insensitive molecular probes. *Org Lett* 2006;8:581–584.

5. Phillips KM, Ruggio DM, Ashraf-Khorassani M: Phytosterol composition of nuts and seeds commonly consumed in the United States. *J Agric Food Chem* 2005;53:9436–9445.

6. Zhang JH, Chung TD, Oldenburg KR: A simple statistical parameter for use in evaluation and validation of high throughput screening assays. *J Biomol Screen* 1999;4:67–73.

7. Schroeder F, Jefferson JR, Kier AB, Knittel J, Scallen TJ, Wood WG, *et al.*: Membrane cholesterol dynamics: cholesterol domains and kinetic pools. *Proc Soc Exp Biol Med* 1991;196:235–252.

8. Schroeder F, Woodford JK, Kavecansky J, Wood WG, Joiner C: Cholesterol domains in biological membranes. *Mol Membr Biol* 1995;12:113–119.

9. Avdulov NA, Chochina SV, Igbavboa U, Wood WG: Cholesterol efflux to high-density lipoproteins and apolipoprotein A-I phosphatidylcholine complexes is inhibited by ethanol: role of apolipoprotein structure and cooperative interaction of phosphatidylcholine and cholesterol. *Biochemistry* 2000;39:10599–10606.

10. Sparrow CP, Patel S, Baffic J, Chao YS, Hernandez M, Lam MH, *et al.*: A fluorescent cholesterol analog traces cholesterol absorption in hamsters and is esterified *in vivo* and *in vitro*. *J Lipid Res* 1999;40:1747–1757.

11. Frolov A, Petrescu A, Atshaves BP, So PT, Gratton E, Serrero G, *et al.*: High density lipoprotein-mediated cholesterol uptake and targeting to lipid droplets in intact L-cell fibroblasts. A single- and multiphoton fluorescence approach. *J Biol Chem* 2000;275:12769–12780.

12. Portioli Silva EP, Peres CM, Roberto Mendonca J, Curi R: NBD-cholesterol incorporation by rat macrophages and lymphocytes: a process dependent on the activation state of the cells. *Cell Biochem Funct* 2004;22:23–28.

13. Lee TS, Pan CC, Peng CC, Kou YR, Chen CY, Ching LC, *et al.*: Anti-atherogenic effect of berberine on LXRalpha-ABCA1-dependent cholesterol efflux in macrophages. *J Cell Biochem* 2010 [Epub ahead of print].

14. Atshaves BP, Starodub O, McIntosh A, Petrescu A, Roths JB, Kier AB, *et al.*: Sterol carrier protein-2 alters high density lipoprotein-mediated cholesterol efflux. *J Biol Chem* 2000;275:36852–36861.

15. Duffy D, Rader DJ: Emerging therapies targeting high-density lipoprotein metabolism and reverse cholesterol transport. *Circulation* 2006;113:1140–1150.

16. Mencarelli A, Renga B, Distrutti E, Fiorucci S: Antiatherosclerotic effect of farnesoid X receptor. *Am J Physiol Heart Circ Physiol* 2009;296:H272–H281.

17. Guo GL, Santamarina-Fojo S, Akiyama TE, Amar MJ, Paigen BJ, Brewer B, Jr., *et al.*: Effects of FXR in foam-cell formation and atherosclerosis development. *Biochim Biophys Acta* 2006;1761:1401–1409.

18. Zhang Y, Wang X, Vales C, Lee FY, Lee H, Lusis AJ, *et al.*: FXR deficiency causes reduced atherosclerosis in Ldlr−/−mice. *Arterioscler Thromb Vasc Biol* 2006; 26:2316–2321.

19. Griel AE, Kris-Etherton PM: Tree nuts and the lipid profile: a review of clinical studies. *Br J Nutr* 2006;96 Suppl 2:S68–S78.

20. Zhao G, Etherton TD, Martin KR, West SG, Gillies PJ, Kris-Etherton PM: Dietary alpha-linolenic acid reduces inflammatory and lipid cardiovascular risk factors in hypercholesterolemic men and women. *J Nutr* 2004;134:2991–2997.

21. Zhao G, Etherton TD, Martin KR, Vanden Heuvel JP, Gillies PJ, West SG, *et al.*: Anti-inflammatory effects of polyunsaturated fatty acids in THP-1 cells. *Biochem Biophys Res Commun* 2005;336:909–917.

22. Zhao G, Etherton TD, Martin KR, Gillies PJ, West SG, Kris-Etherton PM: Dietary alpha-linolenic acid inhibits proinflammatory cytokine production by peripheral blood mononuclear cells in hypercholesterolemic subjects. *Am J Clin Nutr* 2007;85:385–391.

23. USDA: USDA National Nutrient Database for Standard Reference, Release 22. Available at www.nal.usda.gov/fnic/foodcomp/search/, accessed January 18, 2010.

24. Nishimoto T, Pellizzon MA, Aihara M, Stylianou IM, Billheimer JT, Rothblat G, *et al.*: Fish oil promotes macrophage reverse cholesterol transport in mice. *Arterioscler Thromb Vasc Biol* 2009;29:1502–1508.

25. Brown JM, Chung S, Sawyer JK, Degirolamo C, Alger HM, Nguyen TM, *et al.*: Combined therapy of dietary fish oil and stearoyl-CoA desaturase 1 inhibition prevents the metabolic syndrome and atherosclerosis. *Arterioscler Thromb Vasc Biol* 2010;30:24–30.

26. Smith JD, Miyata M, Ginsberg M, Grigaux C, Shmookler E, Plump AS: Cyclic AMP induces apolipoprotein E binding activity and promotes cholesterol efflux from a macrophage cell line to apolipoprotein acceptors. *J Biol Chem* 1996;271:30647–30655.

27. Sakr SW, Williams DL, Stoudt GW, Phillips MC, Rothblat GH: Induction of cellular cholesterol efflux to lipid-free apolipoprotein A-I by cAMP. *Biochim Biophys Acta* 1999;1438:85–98.

28. Oram JF, Mendez AJ, Lymp J, Kavanagh TJ, Halbert CL: Reduction in apolipoprotein-mediated removal of cellular lipids by immortalization of human fibroblasts and its reversion by cAMP: lack of effect with Tangier disease cells. *J Lipid Res* 1999;40:1769–1781.

29. Costet P, Luo Y, Wang N, Tall AR: Sterol-dependent transactivation of the ABC1 promoter by the liver X receptor/retinoid X receptor. *J Biol Chem* 2000; 275:28240–28245.

30. Oram JF, Vaughan AM: ATP-binding cassette cholesterol transporters and cardiovascular disease. *Circ Res* 2006;99:1031–1043.

31. Tall AR: Cholesterol efflux pathways and other potential mechanisms involved in the athero-protective effect of high density lipoproteins. *J Intern Med* 2008;263:256–273.

32. Fielding PE, Nagao K, Hakamata H, Chimini G, Fielding CJ: A two-step mechanism for free cholesterol and phospholipid efflux from human vascular cells to apolipoprotein A-1. *Biochemistry* 2000;39:14113–14120.

33. Nieland TJ, Chroni A, Fitzgerald ML, Maliga Z, Zannis VI, Kirchhausen T, *et al.*: Cross-inhibition of SR-BI- and ABCA1-mediated cholesterol transport by the small molecules BLT-4 and glyburide. *J Lipid Res* 2004;45:1256–1265.

34. Abe-Dohmae S, Kato KH, Kumon Y, Hu W, Ishigami H, Iwamoto N, *et al.*: Serum amyloid A generates high density lipoprotein with cellular lipid in an ABCA1- or ABCA7-dependent manner. *J Lipid Res* 2006;47:1542–1550.

35. Mack JT, Beljanski V, Tew KD, Townsend DM: The ATP-binding cassette transporter ABCA2 as a mediator of intracellular trafficking. *Biomed Pharmacother* 2006;60:587–592.

36. Chan SL, Kim WS, Kwok JB, Hill AF, Cappai R, Rye KA, *et al.*: ATP-binding cassette transporter A7 regulates processing of amyloid precursor protein *in vitro. J Neurochem* 2008;106:793–804.

37. Jehle AW, Gardai SJ, Li S, Linsel-Nitschke P, Morimoto K, Janssen WJ, *et al.*: ATP-binding cassette transporter A7 enhances phagocytosis of apoptotic cells and associated ERK signaling in macrophages. *J Cell Biol* 2006;174:547–556.

38. Morales CR, Marat AL, Ni X, Yu Y, Oko R, Smith BT, *et al.*: ATP-binding cassette transporters ABCA1, ABCA7, and ABCG1 in mouse spermatozoa. *Biochem Biophys Res Commun* 2008;376:472–477.

39. Calder PC, Bond JA, Harvey DJ, Gordon S, Newsholme EA: Uptake and incorporation of saturated and unsaturated fatty acids into macrophage lipids and their effect upon macrophage adhesion and phagocytosis. *Biochem J* 1990;269:807–814.

Address correspondence to:
John P. Vanden Heuvel, Ph.D.
Department of Veterinary and Biomedical Sciences
The Pennsylvania State University
325 Life Sciences Building
University Park, PA 16802

E-mail: jpv2@psu.edu